Capturing static and dynamic correlation with ΔNO-MP2 and ΔNO-CCSD

Joshua W. Hollett[1, 2, 3, a)] and Pierre-François Loos[3]

[1)] *Department of Chemistry, University of Winnipeg, Winnipeg, Manitoba, R3B 2G3, Canada*
[2)] *Department of Chemistry, University of Manitoba, Winnipeg, Manitoba, R3T 2N2, Canada*
[3)] *Laboratoire de Chimie et Physique Quantiques (UMR 5626), Université de Toulouse, CNRS, UPS, France*

The ΔNO method for static correlation is combined with second-order Møller-Plesset perturbation theory (MP2) and coupled-cluster singles and doubles (CCSD) to account for dynamic correlation. The MP2 and CCSD expressions are adapted from finite-temperature CCSD, which includes orbital occupancies and vacancies, and expanded orbital summations. Correlation is partitioned with the aid of damping factors incorporated into the MP2 and CCSD residual equations. Potential energy curves for a selection of diatomics are in good agreement with extrapolated full configuration interaction results (exFCI), and on par with conventional multireference approaches.

I. INTRODUCTION

The correlation problem persists. To state it simply; how does one adequately account for electron correlation with a minimal amount of effort? Its persistence is ensured by the latter condition. This continual search for an efficient treatment of electron correlation is driven by the need to treat larger and more complex systems with increased accuracy. A common strategy of potential solutions is the partitioning of the problem into different types of correlation; static and dynamic,[1–11] long-range and short-range,[12–16] *etc.* Partitioning the correlation problem into static and dynamic correlation, or strong and weak correlation, or multireference and "the rest", is a popular and effective strategy that generally provides a qualitative, and sometimes quantitative, model for particularly challenging electronic structure problems. The price of the success of such models is relatively expensive calculations, often combined with the non-trivial definition of active spaces that requires both chemical intuition and trial-and-error. Through the reformulation of these problems in terms of alternative models of electronic structure, a deeper and more "physical" understanding of correlation partitioning can be achieved while providing another tool for the study of complex multireference systems.

A two-tiered wave function based approach to static and dynamic correlation is a relatively old idea.[17–21] The general strategy of manually (or automatically[22,23]) defining an active space, optimizing a multireference wave function, and then applying some form of post-Hartree-Fock electron correlation method, is the basis of a multitude of multireference electronic structure models.[21,24–26] These models have continually evolved over the decades, and prominently include CASPT2,[19,27,28] NEVPT,[29–31] MRCC,[17,18,32,33] and NOCI.[34–37] These methods are essentially the default for studying systems with low-lying excited states (*e.g.*, conical intersections), largely because conventional density functional methods often fail to properly model

such systems. An emerging alternative to these approaches, particularly for describing the multireference aspect, is cumulant functional methods [*e.g.*, density-matrix functional theory (DMFT)[38–45] and natural orbital functional theory (NOFT)[46–53])]. Recently, a two-tiered approach as seen in wave function approaches was devised for NOFT by Piris, NOF-MP2.[53,54] Other than NOF-MP2, the combination of a cumulant functional for static correlation and post-Hartree-Fock theories for dynamic correlation is unexplored.

Upon its inception, the ΔNO method[8] involved employing a cumulant functional to account for static correlation (or multireference character) in conjunction with an on-top density functional for dynamic correlation. The on-top density functional is applied directly to the statically correlated ΔNO two-electron density matrix (2-RDM), therefore the method for treating dynamic correlation can be easily substituted. Recently, White and Chan introduced a finite-temperature formulation of the coupled-cluster approximation (FT-CCSD)[55] in which orbitals are thermally populated according to a Fermi-Dirac distribution, therefore there are non-integer electron occupancies and vacancies (holes). Similar formulations also exist for second-order Møller-Plesset perturbation theory (FT-MP2).[56,57] The finite-temperature formulations of post-Hartree-Fock approaches present an ideal framework for treating the dynamic correlation of a multireference (or statically correlated) 2-RDM obtained from ΔNO, or elsewhere.

The method presented here involves combining ΔNO for static correlation with MP2 or CCSD for dynamic correlation, by exploiting aspects of the finite-temperature formulation. The combination is made possible by introducing a Δ-dependent damping factor in the leading term of the MP2 or CCSD residuals, which modifies the occupancy-occupancy, vacancy-vacancy, and occupancy-vacancy pairs according to the amount of static correlation present. The ΔNO method is introduced in Subsec. II A, the modified MP2 and CCSD equations are described in Subsecs. II C and II B, and the damping factors are defined in Appendix A. The implementation of the method is described in Sec. III and results for the dissociation of some diatomics are presented and discussed in Sec. IV. Finally, some conclusions regarding the current

———————
a)Corresponding author: j.hollett@uwinnipeg.ca

implementation and some future directions are discussed in Sec. V. Atomic units are used throughout unless stated otherwise.

II. THEORY

A. ΔNO method

Cumulant functional theory (CFT) is based on the cumulant expansion of the exact two-electron reduced density matrix (2-RDM) in terms of the one-electron reduced density matrix (1-RDM) and occasionally other variables.[58] The 2-RDM can be defined in terms of the N-electron wave function,

$$\tilde{\Gamma}(\mathbf{x}_1, \mathbf{x}_2, \mathbf{x}_1', \mathbf{x}_2') = \frac{N(N-1)}{2} \int \Psi^*(\mathbf{x}_1', \mathbf{x}_2', \mathbf{x}_3, \dots, \mathbf{x}_N)$$
$$\times \Psi(\mathbf{x}_1, \mathbf{x}_2, \mathbf{x}_3, \dots, \mathbf{x}_N) d\mathbf{x}_3 \dots d\mathbf{x}_N, \quad (1)$$

where $\mathbf{x} = (\mathbf{r}, \omega)$ represents both the spatial and spin coordinates of an electron. The 1-RDM follows from the 2-RDM via integration of the coordinates of one of the electrons,

$$\tilde{\gamma}(\mathbf{x}, \mathbf{x}') = \frac{2}{N-1} \int \tilde{\Gamma}(\mathbf{x}, \mathbf{x}_2, \mathbf{x}', \mathbf{x}_2) d\mathbf{x}_2. \quad (2)$$

The cumulant expansion of the 2-RDM can be written as

$$\tilde{\Gamma}(\mathbf{x}_1, \mathbf{x}_2, \mathbf{x}_1', \mathbf{x}_2')$$
$$= \tilde{\Gamma}^{(0)}(\mathbf{x}_1, \mathbf{x}_2, \mathbf{x}_1', \mathbf{x}_2') + \tilde{\Gamma}_{\text{cum}}(\mathbf{x}_1, \mathbf{x}_2, \mathbf{x}_1', \mathbf{x}_2'), \quad (3)$$

where the zeroth-order term of the expansion, $\tilde{\Gamma}^{(0)}$, is expressed solely in terms of the 1-RDM,

$$\tilde{\Gamma}^{(0)}(\mathbf{x}_1, \mathbf{x}_2, \mathbf{x}_1', \mathbf{x}_2')$$
$$= \frac{1}{2}[\tilde{\gamma}(\mathbf{x}_1, \mathbf{x}_1')\tilde{\gamma}(\mathbf{x}_2, \mathbf{x}_2') - \tilde{\gamma}(\mathbf{x}_1, \mathbf{x}_2')\tilde{\gamma}(\mathbf{x}_2, \mathbf{x}_1')]. \quad (4)$$

The general form of the cumulant, $\tilde{\Gamma}_{\text{cum}}$, for an N-electron system is unknown, and present CFT methods are distinguished by how they approximate this term. When $\tilde{\Gamma}_{\text{cum}}$ is constructed exclusively from the natural orbitals (NOs), $\{\phi_p\}$, and their occupancies, $\{n_p\}$, (which are the eigenfunctions and eigenvalues of the 1-RDM, respectively) a natural orbital functional (NOF) is the result. For notational convenience, we also define natural vacancies as $h_p = 1 - n_p$ and assume real-valued NOs. Unlike NOFs, the ΔNO method uses electron transfer variables, $\{\Delta_{me}\}$, which correspond to the amount of electron occupancy transferred from an "occupied" active orbital ϕ_m to a "virtual" active orbital ϕ_e. Note that "occupied" and "virtual" designations refer to the ground-state Hartree-Fock electron configuration[8] (see Table I for orbital labelling).

TABLE I. Orbital index key for ΔNO, MP2 and CCSD.

indices	orbitals	trait	set label
p, q, r, s	all		
i, j, k, l	occupied	$n_i \neq 0$	$\mathcal{O}$
a, b, c, d	virtual	$h_a \neq 0$	$\mathcal{V}$
m, n	active occupied	$n_m < 1$	$\mathcal{A}_o$
e, f	active virtual	$h_e < 1$	$\mathcal{A}_v$

In ΔNO, the occupancies are defined in terms of these variational $\{\Delta_{me}\}$,

$$n_m = 1 - \sum_e \Delta_{me}, \qquad n_e = \sum_m \Delta_{me}. \quad (5)$$

Further distinguishing the ΔNO functional from NOFs, or other cumulant functionals, is that the transfer of electrons occurs between a relatively small set of active occupied, $\mathcal{A}_o = \{\phi_m\}$, and virtual, $\mathcal{A}_v = \{\phi_e\}$, orbitals. This is because the ΔNO cumulant functional is designed to capture only static correlation.

For this work, it is useful to describe the spinless, spin-resolved, ΔNO 2-RDM. In general, the spinless 2-RDM is obtained by integrating over the spin of the two electrons,

$$\Gamma(\mathbf{r}_1, \mathbf{r}_2, \mathbf{r}_1', \mathbf{r}_2') = \iint \tilde{\Gamma}(\mathbf{x}_1, \mathbf{x}_2, \mathbf{x}_1', \mathbf{x}_2')\Big|_{\substack{\omega_1' = \omega_1 \\ \omega_2' = \omega_2}} d\omega_1 d\omega_2. \quad (6)$$

The result can then be resolved into the components associated with different spin-pairs,

$$\Gamma(\mathbf{r}_1, \mathbf{r}_2, \mathbf{r}_1', \mathbf{r}_2') = \Gamma^{\uparrow\uparrow}(\mathbf{r}_1, \mathbf{r}_2, \mathbf{r}_1', \mathbf{r}_2') + \Gamma^{\downarrow\downarrow}(\mathbf{r}_1, \mathbf{r}_2, \mathbf{r}_1', \mathbf{r}_2')$$
$$+ \Gamma^{\uparrow\downarrow}(\mathbf{r}_1, \mathbf{r}_2, \mathbf{r}_1', \mathbf{r}_2') + \Gamma^{\downarrow\uparrow}(\mathbf{r}_1, \mathbf{r}_2, \mathbf{r}_1', \mathbf{r}_2'). \quad (7)$$

Furthermore, the 2-RDM can also be expanded in the basis of the NOs,

$$\Gamma(\mathbf{r}_1, \mathbf{r}_2, \mathbf{r}_1', \mathbf{r}_2') = \sum_{pqrs} \Gamma_{pqrs} \phi_p(\mathbf{r}_1')\phi_q(\mathbf{r}_2')\phi_r(\mathbf{r}_1)\phi_s(\mathbf{r}_2). \quad (8)$$

For a closed-shell system, the zeroth-order term of the cumulant expansion becomes

$$\left(\Gamma^{(0),\sigma\sigma}\right)_{pqrs} = \frac{n_p n_q}{2} \delta_{pr}^{qs}, \quad (9a)$$

$$\left(\Gamma^{(0),\sigma\sigma'}\right)_{pqrs} = \frac{n_p n_q}{2} \delta_{pr}\delta_{qs}, \quad (9b)$$

where $\delta_{pr}^{qs} = \delta_{pr}\delta_{qs} - \delta_{ps}\delta_{qr}$, $n_p = n_p^\uparrow = n_p^\downarrow$ and $\sigma, \sigma' = \uparrow$ or $\downarrow$.

The ΔNO cumulant consists of three terms,

$$\Gamma_{\text{cum}}^{\Delta\text{NO}} = \Gamma_{\text{pair}}^{\Delta\text{NO}} + \Gamma_{\text{stat}}^{\Delta\text{NO}} + \Gamma_{\text{HSC}}^{\Delta\text{NO}}, \quad (10)$$

a pair correction term, $\Gamma_{\text{pair}}^{\Delta\text{NO}}$, a static correlation term, $\Gamma_{\text{stat}}^{\Delta\text{NO}}$, and a high-spin correction term, $\Gamma_{\text{HSC}}^{\Delta\text{NO}}$, where each can be decomposed into its spin-pair components.

For non-integer occupancies, $\Gamma^{(0)}$ [see Eq. (9)] does not integrate to the total number of electron pairs, $N(N-1)/2$. The pair correction term, $\Gamma^{\Delta\text{NO}}_{\text{pair}}$, ensures the total 2-RDM integrates to this number for any $\{\Delta_{me}\}$, and is given as

$$\left(\Gamma^{\Delta\text{NO},\sigma\sigma}_{\text{pair}}\right)_{pqrs} = \frac{\Delta_{pq}(n_q - n_p - \Delta_{pq}) - \eta_{pq}}{2}\delta^{qs}_{pr}, \quad (11\text{a})$$

$$\left(\Gamma^{\Delta\text{NO},\sigma\sigma'}_{\text{pair}}\right)_{pqrs} = \frac{n_p h_p}{2}\delta_{pq}\delta_{pr}\delta_{qs}$$
$$+ \frac{\Delta_{pq}(n_q - n_p - \Delta_{pq}) - \eta_{pq}}{2}\delta_{pr}\delta_{qs}, \quad (11\text{b})$$

where

$$\eta_{pq} = \begin{cases} \sum_r \Delta_{pr}\Delta_{qr}, & \text{if } p \neq q \wedge (\phi_p, \phi_q) \in \mathcal{A}_o \\ & \text{or } p \neq q \wedge (\phi_p, \phi_q) \in \mathcal{A}_v, \\ 0, & \text{otherwise}, \end{cases} \quad (12)$$

and $\Delta_{pq} = -\Delta_{qp}$.

In the framework of ΔNO, static correlation is captured by transferring opposite-spin electron pairs from the same active occupied NO, ϕ_m, to the same active virtual NO, ϕ_e. This recovers the same intrapair correlation as the $2n$-tuple excitations of a seniority-zero configuration interaction wave function,[59,60] for which excitations are performed only within a relatively small active space.

The static correlation term of the cumulant is written as

$$\left(\Gamma^{\Delta\text{NO},\sigma\sigma}_{\text{stat}}\right)_{pqrs} = 0, \quad (13\text{a})$$

$$\left(\Gamma^{\Delta\text{NO},\sigma\sigma'}_{\text{stat}}\right)_{pqrs} = \frac{\zeta_{pr} - \tau_{pr}}{2}\delta_{pq}\delta_{rs}, \quad (13\text{b})$$

where

$$\zeta_{pq} = \begin{cases} \sum_r \sqrt{\Delta_{pr}\Delta_{qr}}, & \text{if } p \neq q \wedge (\phi_p, \phi_q) \in \mathcal{A}_o \\ & \text{or } p \neq q \wedge (\phi_p, \phi_q) \in \mathcal{A}_v, \\ 0, & \text{otherwise}, \end{cases} \quad (14)$$

and

$$\tau_{pq} = \begin{cases} \sqrt{n_p \Delta_{pq}}, & \text{if } \phi_p \in \mathcal{A}_o \wedge \phi_q \in \mathcal{A}_v, \\ \sqrt{n_q \Delta_{qp}}, & \text{if } \phi_p \in \mathcal{A}_v \wedge \phi_q \in \mathcal{A}_o, \\ 0, & \text{otherwise}. \end{cases} \quad (15)$$

Like a seniority-zero wave function, no parallel-spin correlation is included in the static correlation term. However, the high-spin correction (HSC) includes interpair, opposite- and parallel-spin, correlation that is not present in a seniority-zero wave function. This correlation is necessary for the proper dissociation of multiple bonds into high-spin fragments, and for the static correlation of multiple electron pairs in general.[43] The HSC term is written as

$$\left(\Gamma^{\Delta\text{NO},\sigma\sigma}_{\text{HSC}}\right)_{pqrs} = \frac{\kappa_{pq}}{2}\delta^{qs}_{pr}, \quad (16\text{a})$$

$$\left(\Gamma^{\Delta\text{NO},\sigma\sigma'}_{\text{HSC}}\right)_{pqrs} = -\frac{\kappa_{pq}}{2}\delta_{pr}\delta_{qs}, \quad (16\text{b})$$
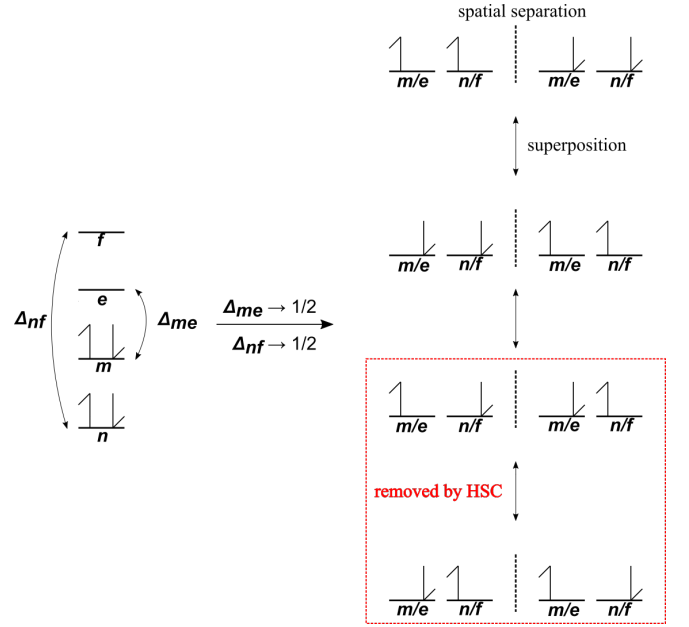

FIG. 1. Diagrammatic representation of the ΔNO high-spin correction (HSC) for two statically correlated electron pairs. Without the HSC, at complete static correlation ($\Delta = 1/2$), the ΔNO 2-RDM would contain a superposition of four different spin configurations about a spatial separation [dashed line] (e.g., dissociated atoms). The HSC removes the "low-spin" configurations, leaving only the "high-spin" configurations.

where

$$\kappa_{pq} = \begin{cases} \sum_{\substack{r \neq s \\ (r \neq q) \\ (s \neq p)}} \tau_{pr}\tau_{qs}, & \text{if } p \neq q \wedge (\phi_p, \phi_q) \in \mathcal{A}, \\ 0, & \text{otherwise}. \end{cases} \quad (17)$$

The HSC reduces the pair density between opposite-spin electrons, while increasing the pair density between parallel-spin electrons, of separate statically correlated electron pairs, as their static correlation increases. This is illustrated in Fig. 1 for two statically correlated electron pairs. Taking N_2 dissociation as an example, the HSC ensures that the spin-up electrons of each of the three statically correlated pairs (triple bond) simultaneously appear on one atom while the spin-down electrons appear on the other, resulting in a superposition of the two high-spin fragment possibilities. Without the correction, the electrons of each statically correlated pair would encounter an average of both parallel and opposite-spin electrons from the other statically correlated pairs (i.e., spin-averaged).

The total ΔNO energy follows simply from the 2-RDM,

$$E^{\Delta\text{NO}} = E^{(0)} + E^{\Delta\text{NO}}_{\text{cum}}, \quad (18)$$

where the zeroth-order 1-RDM energy also includes the one-electron, kinetic and electron-nucleus attraction, energy in addition to the two-electron energy associated with the zeroth-order term of the cumulant expansion,

$\Gamma^{(0)}$. For a closed-shell system, the zeroth-order 1-RDM energy, in terms of NOs and occupancies, is given as

$$E^{(0)} = 2\sum_p n_p H_p + \sum_{pq} n_p n_q (2J_{pq} - K_{pq}), \qquad (19)$$

where

$$H_p = \int \phi_p(\mathbf{r})\left(-\frac{\nabla^2}{2} - \sum_A \frac{Z_A}{r_A}\right)\phi_p(\mathbf{r})d\mathbf{r}, \qquad (20a)$$

$$J_{pq} = \iint \frac{\phi_p(\mathbf{r}_1)\phi_q(\mathbf{r}_2)\phi_p(\mathbf{r}_1)\phi_q(\mathbf{r}_2)}{r_{12}}d\mathbf{r}_1 d\mathbf{r}_2, \qquad (20b)$$

$$K_{pq} = \iint \frac{\phi_p(\mathbf{r}_1)\phi_q(\mathbf{r}_2)\phi_q(\mathbf{r}_1)\phi_p(\mathbf{r}_2)}{r_{12}}d\mathbf{r}_1 d\mathbf{r}_2, \qquad (20c)$$

are the usual one-electron (kinetic and nuclear attraction) and two-electron (Coulomb and exchange) integrals over NOs. The cumulant energy is given as

$$E_{\text{cum}}^{\Delta\text{NO}} = E_{\text{pair}}^{\Delta\text{NO}} + E_{\text{stat}}^{\Delta\text{NO}} + E_{\text{HSC}}^{\Delta\text{NO}} + E_{\text{dyn}}^{\Delta\text{NO}}, \qquad (21)$$

with components defined as follows

$$\begin{aligned} E_{\text{pair}}^{\Delta\text{NO}} &= \sum_p n_p h_p J_{pp} \\ &+ \sum_{pq} \Delta_{pq}(n_q - n_p - \Delta_{pq})(2J_{pq} - K_{pq}) \\ &- \sum_{pq} \eta_{pq}(2J_{pq} - K_{pq}), \end{aligned} \qquad (22a)$$

$$E_{\text{stat}}^{\Delta\text{NO}} = \sum_{pq}(\zeta_{pq} - \tau_{pq})L_{pq}, \qquad (22b)$$

$$E_{\text{HSC}}^{\Delta\text{NO}} = -\sum_{pq}\kappa_{pq}K_{pq}, \qquad (22c)$$

where the time-inversion exchange energy integrals are

$$L_{pq} = \iint \frac{\phi_p(\mathbf{r}_1)\phi_p(\mathbf{r}_2)\phi_q(\mathbf{r}_1)\phi_q(\mathbf{r}_2)}{r_{12}}d\mathbf{r}_1 d\mathbf{r}_2. \qquad (23)$$

The HSC energy appears simplified in comparison to the 2-RDM term [see Eq. (16)]. This is because the Coulomb repulsion terms cancel due to the equivalence of the spin-up and spin-down NOs. The dynamic correlation energy, $E_{\text{dyn}}^{\Delta\text{NO}}$, was defined previously in terms of an on-top density functional.[8] In the present study the dynamic correlation energy is provided via MP2 or CCSD, *i.e.*,

$$E_{\text{dyn}}^{\Delta\text{NO}} = E_{\text{MP2/CCSD}}^{\Delta\text{NO}}. \qquad (24)$$

B. CCSD for ΔNO

Recently, White and Chan introduced a finite-temperature formulation of the coupled-cluster singles and doubles method (FT-CCSD).[55] The method is formulated in terms of imaginary time, which is integrated from 0 to β, where β is the inverse temperature. The authors state that at zero temperature, the FT-CCSD amplitudes, and consequently the energy, converge to the usual non-temperature dependent CCSD values. In that case, the electron occupancies, which are determined by a Fermi-Dirac distribution, would collapse to their normal Aufbau (Hartree-Fock ground state) values. For ΔNO, the occupancies are not those of Aufbau or the Fermi-Dirac distribution, nevertheless it is assumed here that aspects of the FT-CCSD formulation are still valid. In their article, White and Chan outline how to convert CC equations (*i.e.*, residuals) to FT-CC equations. The equations presented here are formulated by taking the CCSD equations of Stanton *et al.*[61] and applying the instructions from White and Chan to include occupancies and vacancies (holes). The necessary instructions (paraphrased) being: (i) for each contraction, sum over all orbitals instead of just occupied or virtual orbitals, and (ii) include an occupancy or vacancy with each index not associated with an amplitude. Application of these instructions to the residual (r_i^a and r_{ij}^{ab}) equations of Stanton *et al.* gives

$$\begin{aligned} r_i^a(\text{CCSD}) &= n_i h_a s_i^a F_{ia} + \sum_c t_i^c \mathcal{F}_{ac} - \sum_k t_k^a \mathcal{F}_{ki} \\ &+ \sum_{kc} t_{ik}^{ac}\mathcal{F}_{kc} - \sum_{kc} t_k^c \langle ka||ic\rangle n_i h_a \\ &- \frac{1}{2}\sum_{kcd} t_{ik}^{cd}\langle ka||cd\rangle h_a \\ &- \frac{1}{2}\sum_{klc} t_{kl}^{ac}\langle lk||ci\rangle n_i, \end{aligned} \qquad (25)$$

and

$$\begin{aligned} r_{ij}^{ab}(\text{CCSD}) &= n_i n_j h_a h_b d_{ij}^{ab}\langle ij||ab\rangle \\ &+ P_{ab}\sum_c t_{ij}^{ac}\left(\mathcal{F}_{bc} - \frac{1}{2}\sum_k t_k^b \mathcal{F}_{kc}\right) \\ &- P_{ij}\sum_k t_{ik}^{ab}\left(\mathcal{F}_{kj} + \frac{1}{2}\sum_c t_j^c \mathcal{F}_{kc}\right) \\ &+ \frac{1}{2}\sum_{kl}\tau_{kl}^{ab}\mathcal{W}_{klij} + \frac{1}{2}\sum_{cd}\tau_{ij}^{cd}\mathcal{W}_{abcd} \\ &+ P_{ij}P_{ab}\sum_{kc}(t_{ik}^{ac}\mathcal{W}_{kbcj} - t_i^c t_k^a \langle kb||cj\rangle h_b n_j) \\ &+ P_{ij}\sum_c t_i^c \langle ab||cj\rangle n_j h_a h_b \\ &- P_{ab}\sum_k t_k^a \langle kb||ij\rangle n_i n_j h_b, \end{aligned} \qquad (26)$$

where P is a permutation operator such that $P_{ij}g_{ij} = g_{ij} - g_{ji}$. The various matrix elements from Eqs. (25)

and (26) read

$$\mathcal{F}_{ac} = h_a F_{ac} - \frac{1}{2} \sum_k t_k^a F_{kc}$$
$$+ \sum_{kd} t_k^d \langle ka||dc \rangle h_a - \frac{1}{2} \sum_{kld} \tilde{\tau}_{kl}^{ad} \langle kl||cd \rangle , \quad (27a)$$

$$\mathcal{F}_{ki} = n_i F_{ik} + \frac{1}{2} \sum_c t_i^c F_{kc}$$
$$+ \sum_{cl} t_l^c \langle kl||ic \rangle n_i + \frac{1}{2} \sum_{lcd} \tilde{\tau}_{il}^{cd} \langle kl||cd \rangle , \quad (27b)$$

$$\mathcal{F}_{kc} = F_{kc} + \sum_{ld} t_l^d \langle kl||cd \rangle , \quad (27c)$$

and

$$\mathcal{W}_{klij} = n_i n_j \langle kl||ij \rangle$$
$$+ P_{ij} \sum_c t_j^c \langle kl||ic \rangle n_i + \frac{1}{4} \sum_{cd} \tau_{ij}^{cd} \langle kl||cd \rangle , \quad (28a)$$

$$\mathcal{W}_{abcd} = h_a h_b \langle ab||cd \rangle$$
$$- P_{ab} \sum_k t_k^b \langle ak||cd \rangle h_a + \frac{1}{4} \sum_{kl} \tau_{kl}^{ab} \langle kl||cd \rangle , \quad (28b)$$

$$\mathcal{W}_{kbcj} = h_b n_j \langle kb||cj \rangle$$
$$+ \sum_d t_j^d \langle kb||cd \rangle h_b - \sum_l t_l^b \langle kl||cj \rangle n_j$$
$$- \sum_{ld} \left(\frac{t_{jl}^{db}}{2} + t_j^d t_l^b \right) \langle kl||cd \rangle , \quad (28c)$$

where we have defined the intermediate quantities

$$\tau_{ij}^{ab} = t_{ij}^{ab} + t_i^a t_j^b - t_i^b t_j^a, \quad (29a)$$

$$\tilde{\tau}_{ij}^{ab} = t_{ij}^{ab} + \frac{1}{2}\left(t_i^a t_j^b - t_i^b t_j^a\right). \quad (29b)$$

The element

$$F_{pq} = \frac{1}{n_p} \int \frac{\delta\left(E^{(0)} + E_{\text{pair}}^{\Delta\text{NO}}\right)}{\delta\chi_p(\mathbf{x})} \chi_q(\mathbf{x}) d\mathbf{x} \quad (30)$$

denotes a generalized ΔNO Fock matrix element, where $\chi_p(\mathbf{x})$ is a natural spin-orbital. The antisymmetrized electron repulsion integrals are given by $\langle pq||rs \rangle = \langle pq|rs \rangle - \langle pq|sr \rangle$ with

$$\langle pq|rs \rangle = \int \frac{\chi_p(\mathbf{x}_1)\chi_q(\mathbf{x}_2)\chi_r(\mathbf{x}_1)\chi_s(\mathbf{x}_2)}{r_{12}} d\mathbf{x}_1 d\mathbf{x}_2. \quad (31)$$

Besides introducing occupancies and vacancies, and expanding the range of the sums over spin-orbitals, one more modification is applied to both the r_i^a and r_{ij}^{ab} equations. The leading term of each residual equation is multiplied by a damping factor (s_i^a for r_i^a and d_{ij}^{ab} for r_{ij}^{ab}), which are defined in Appendix A. The CCSD energy expression is unmodified, with the exception of the range of summation,

$$E_{\text{CCSD}}^{\Delta\text{NO}} = \sum_{ia} t_i^a F_{ia} + \frac{1}{2} \sum_{ijab} \left(\frac{t_{ij}^{ab}}{2} - t_i^a t_j^b \right) \langle ij||ab \rangle . \quad (32)$$

C. MP2 for ΔNO

An equation for the MP2 amplitudes is derived in a manner analogous to CCSD, where the two instructions of White and Chan [see Subsec. II B] are applied to the usual non-canonical MP2 residual equation,

$$r_{ij}^{ab}(\text{MP2}) = n_i n_j h_a h_b d_{ij}^{ab} \langle ij||ab \rangle$$
$$+ \sum_c \left(h_b t_{ij}^{ac} F_{bc} + h_a t_{ij}^{cb} F_{ac} \right)$$
$$- \sum_k \left(n_j t_{ik}^{ab} F_{jk} + n_i t_{kj}^{ab} F_{ik} \right), \quad (33)$$

where, in addition to the introduction of occupancies and vacancies, and the expanded range of summation, the same damping factor (defined in Appendix A) applied to the CCSD r_{ij}^{ab} equation [see Eq. (26)] is applied here. Also like CCSD, the MP2 energy expression remains the same with the exception of the expanded range of summation, *i.e.*,

$$E_{\text{MP2}}^{\Delta\text{NO}} = \frac{1}{4} \sum_{ijab} t_{ij}^{ab} \langle ij||ab \rangle . \quad (34)$$

Note that because the non-canonical formulation of MP2[62] is employed, Eqs. (33) and (34) do not involve single excitations.

III. METHOD

A. FCI reference

Benchmark potential energy curves were obtained using a determinant-driven selected configuration interaction (sCI) method known as CIPSI (Configuration Interaction using a Perturbative Selection made Iteratively)[63–65] in which the energies are extrapolated to the full configuration interaction (FCI) result using multireference perturbation theory.[66–68] The all-electron extrapolated-FCI (exFCI) calculations were performed using Quantum Package 2.0.[68] All benchmark and ΔNO calculations were performed using the cc-pVTZ/f basis set.[69–72]

B. ΔNO

All ΔNO and subsequent MP2 and CCSD calculations were performed using the MUNgauss quantum chemistry program.[73] Optimization of the $\{\phi_m\}$ and the $\{\Delta_{me}\}$ was performed according to the previously established algorithm.[8,74] Restricted Hartree-Fock orbitals serve as the initial guess NOs, which are then optimized via iterative diagonalization of a pseudo-Fock matrix. The $\{\Delta_{me}\}$ are optimized using a Newton-Raphson algorithm. For the current study, the number of active occupied orbitals

was chosen manually to be the number of bonds in the diatomic. An equivalent number of virtual orbitals were chosen to be active.

C. MP2 and CCSD

Both the MP2 and CCSD algorithms are implemented in the spin-orbital basis. The residual equations are solved using an iterative Newton-Raphson (MP2), or approximate Newton-Raphson (CCSD), approach. Amplitude updates are calculated via

$$t_i^a \leftarrow t_i^a + \frac{r_i^a}{n_i F_{ii} - h_a F_{aa}}, \tag{35a}$$

$$t_{ij}^{ab} \leftarrow t_{ij}^{ab} + \frac{r_{ij}^{ab}}{n_i F_{ii} + n_j F_{jj} - h_a F_{aa} - h_b F_{bb}}, \tag{35b}$$

where the initial t_{ij}^{ab} amplitudes are set to the MP2 values and $t_i^a = 0$. To avoid numerical instabilities, residuals, r_i^a and r_{ij}^{ab}, are considered to be zero if the leading term [see Eqs. (25) and (26) for CCSD, and Eq. (33) for MP2] is below a specific threshold τ,

$$r_i^a = 0, \qquad \text{if } n_i h_a d_i^a F_{ia} < \tau, \tag{36a}$$

$$r_{ij}^{ab} = 0, \qquad \text{if } n_i n_j h_a h_b d_{ij}^{ab} \langle ij||ab \rangle < \tau. \tag{36b}$$

Here τ is set to machine precision. The iterative optimization of the amplitudes is accelerated using a direct inversion of iterative subspace (DIIS) algorithm[75] to extrapolate from amplitudes of previous steps.[76] A maximum number of ten sets of amplitudes from previous steps were kept for extrapolation. In the case of the CCSD iterations, the t_i^a and t_{ij}^{ab} were combined and extrapolated together. Convergence was assumed when the absolute value of the largest residual element was less than 10^{-7}.

IV. RESULTS

The error in the ΔNO-MP2 and ΔNO-CCSD potential energy curves, $U(R)$, for H_2 compared to exFCI is presented in Fig. 2. The potential energy curve is calculated as

$$U(R) = E(R) + V_{nn}(R), \tag{37}$$

where the nuclear repulsion energy, $V_{nn}(R)$, is added to the electronic energy obtained from ΔNO-MP2, ΔNO-CCSD, or exFCI. For H_2, the exFCI result is equivalent to regular FCI, and hence, the exact result for the given basis set. Also, for two electrons, CCSD is equivalent to FCI and therefore any error in $U_{\Delta\text{NO-CCSD}}(R)$ is due to the manner in which the ΔNO static correlation energy is blended with the CCSD dynamic correlation energy. This leads to a maximum error of 1.7 kJ.mol^{-1} at the beginning of the examined range, $R = 1$. There is also
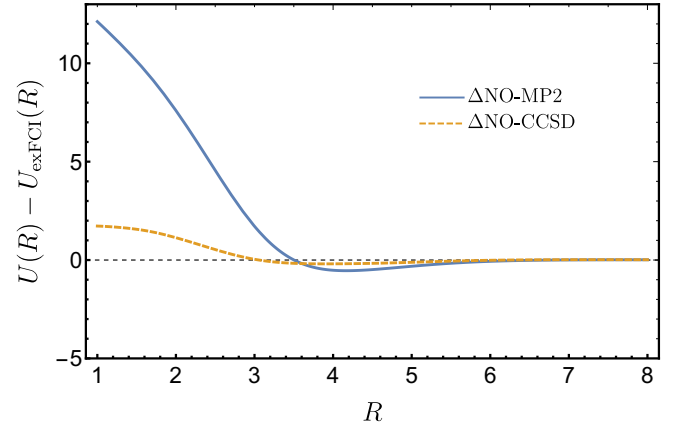

FIG. 2. Error (in kJ.mol^{-1}) in H_2 potential energy curves compared to exFCI. The error in $U_{\text{MP2}}(R)$ is 17 kJ.mol^{-1} at $R = 1$ and continues to grow with increasing R. For H_2, $U_{\text{CCSD}}(R) = U_{\text{exFCI}}(R)$ and therefore the CCSD error is zero for all R.

a slight overestimation of the total correlation energy at stretched bond lengths, with a maximum deviation of -0.2 kJ.mol^{-1} at $R = 3.89$. In the case of ΔNO-MP2, the error at small R is much larger. This can be attributed to the fact that, as $R \to 0$, the correlation energy approaches that of He, for which the MP2 correlation energy differs from the FCI correlation energy by 15.5 kJ.mol^{-1}. As R increases the error in $U_{\Delta\text{NO-MP2}}(R)$ decreases, also with a slight overestimation of correlation energy (-0.5 kJ.mol^{-1} at $R = 4.17$) at stretched bond lengths. For both methods, the damping factors ensure that, as $R \to \infty$, the dynamic correlation energy vanishes, along with the error in $U(R)$.

Equilibrium bond lengths and dissociation energies predicted by ΔNO-MP2 and ΔNO-CCSD for a selection of diatomics, are compared to ΔNO (no dynamic correlation), NOF-MP2[54], MP2, CCSD and exFCI values in Table II. As expected from Fig. 2, the H_2 R_e and D_e values predicted by ΔNO-MP2 and ΔNO-CCSD are very close to the exFCI values. The underestimation of D_e by ΔNO-MP2 is attributable to the lack of dynamic correlation at small to intermediate R. Removal of all of the dynamic correlation, by using ΔNO, results in a much larger underestimation of D_e (by 55 kJ.mol^{-1}). No MP2 D_e value is reported due to the well-known divergence of the potential energy curve to $-\infty$ as R increases. The divergence is due to the degeneracy of the σ-bonding and σ^*-antibonding orbitals of H_2 as $R \to \infty$, and is completely removed in the ΔNO-MP2 treatment.

The ΔNO-MP2, ΔNO-CCSD, MP2, CCSD and exFCI curves for LiH are presented in Fig. 3. Both ΔNO-MP2 and ΔNO-CCSD provide an accurate model of LiH dissociation. Most of the error in $U_{\Delta\text{NO-MP2}}(R)$ occurs near equilibrium, deviating from $U_{\text{exFCI}}(R)$ by 20 kJ.mol^{-1} at $R = 3.028$. Whereas, $U_{\Delta\text{NO-CCSD}}(R)$ only deviates by 3 kJ.mol^{-1} at equilibrium, and 0.2 kJ.mol^{-1} near dissoci-

TABLE II. Calculated equilibrium bond lengths R_e and dissociation energies D_e for a selection of diatomics.

Molecule	R_e (bohr)							D_e (kJ.mol^{-1})						
	exFCI	MP2	CCSD	ΔNO[b]	ΔNO-MP2	ΔNO-CCSD	NOF-MP2[c]	exFCI	MP2[a]	CCSD[a]	ΔNO[b]	ΔNO-MP2	ΔNO-CCSD	NOF-MP2[c]
H$_2$	1.405	1.392	1.405	1.428	1.408	1.405		454		454	399	443	452	
LiH	3.028	3.019	3.027	3.019	3.044	3.030		236	343	238	185	223	233	
HF	1.729	1.731	1.725	1.735	1.741	1.741	1.731	576	667	641	470	603	606	590
LiF	2.981	2.986	2.976	2.946	2.991	2.979	2.984	549	612	610	424	593	582	590
F$_2$	2.692	2.655	2.649	2.779	2.623	2.634	2.612	143		268	67	138	148	192
N$_2$	2.083	2.102	2.069	2.071	2.084	2.077	2.075	880		712	856	891	965	

[a] D_e for potential energy curves with singularities are not reported.
[b] From potential energy curve where $E_{\mathrm{dyn}}^{\Delta\mathrm{NO}} = 0$
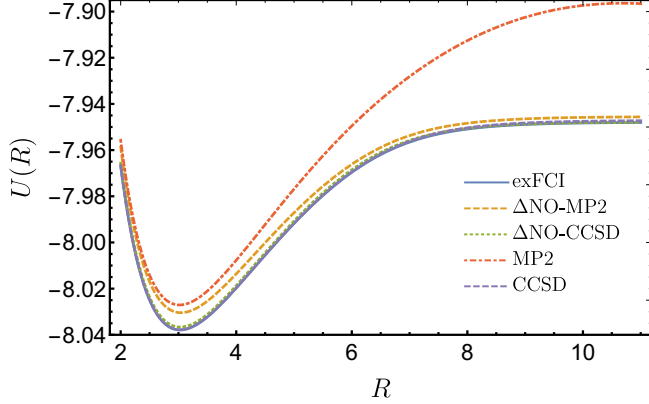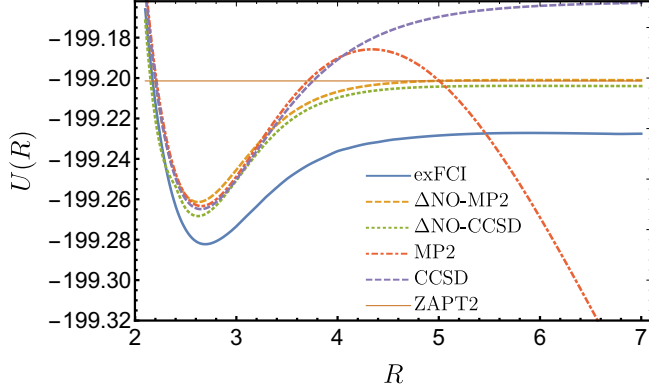[c] Orbital-invariant formulation of NOF-MP2 (NOF-OIMP2/cc-pVTZ) from Piris.[54]

FIG. 3. Calculated LiH potential energy curves.

FIG. 4. Calculated F$_2$ potential energy curves. The ZAPT2 energy of two separate F atoms is included for comparison.

ation, $R = 11$. This means both the static correlation of the LiH bond and dynamic correlation of the electrons on Li are effectively captured by ΔNO-CCSD. Inclusion of only static correlation, via ΔNO, leads to a reasonable prediction of R_e (3.019) but D_e is underestimated by 51 kJ.mol^{-1}.

The potential energy curves for F$_2$ are shown in Fig. 4. Similar to other post-Hartree-Fock correlation methods, ΔNO-MP2 and ΔNO-CCSD struggle to capture the dy-

namic correlation in F$_2$ near equilibrium and in the separated F atoms.[65] This is evident in the large separation between the exFCI curve and all the others. In the case of ΔNO-MP2 and ΔNO-CCSD, the lack of dynamic correlation is relatively consistent and therefore the predicted D_e values are reasonable for both, with ΔNO-MP2 differing from exFCI by -5 kJ.mol^{-1} and ΔNO-CCSD differing by $+5$ kJ.mol^{-1}. The lack of dynamic correlation has a more significant effect on the predicted R_e values, which differ by -0.07 for ΔNO-MP2 and -0.06 for ΔNO-CCSD. The predicted R_e values from MP2 and CCSD also deviate negatively from the exFCI R_e, but the deviation is smaller, approximately -0.04. If dynamic correlation is completely neglected (ΔNO), R_e is significantly overestimated ($+0.09$), and the estimated D_e is exceptionally small, 67 kJ.mol^{-1}.

For a given molecule, the ΔNO energy without dynamic correlation energy (simply referred to as ΔNO in Table II), $E_{\text{no-dyn}}^{\Delta\mathrm{NO}} = E^{(0)} + E_{\text{pair}}^{\Delta\mathrm{NO}} + E_{\text{stat}}^{\Delta\mathrm{NO}} + E_{\text{HSC}}^{\Delta\mathrm{NO}}$, is equivalent to the sum of restricted open-shell Hartree-Fock (ROHF) energies at the bond dissociation limit,

$$\lim_{R\to\infty} E_{\text{no-dyn}}^{\Delta\mathrm{NO}}[\mathrm{A} \overset{\mathrm{R}}{\cdots} \mathrm{B}] = E_{\text{ROHF}}[\mathrm{A}] + E_{\text{ROHF}}[\mathrm{B}]. \quad (38)$$

Therefore, the quality of the ΔNO-MP2 treatment near the bond dissociation limit can be assessed through comparison of the ΔNO-MP2 energy to the ROHF energy plus the z-averaged second-order perturbation energy (ZAPT2)[77] of the two separated fragments. The ZAPT2 energy of two F atoms is plotted in Fig. 4, where it is seen that the ΔNO-MP2 energy is 1.0 kJ.mol^{-1} higher. This confirms that ΔNO-MP2 is correctly capturing and partitioning the static and dynamic correlation energy of F$_2$. This is in sharp contrast to CCSD which drastically overestimates D_e, or MP2 which diverges due to orbital degeneracy. It is clear that, contrary to conventional single-reference methods like MP2 and CCSD, the hybrid ΔNO-MP2 and ΔNO-CCSD methods proposed here are able to accurately model strongly correlated systems.

Similar to F$_2$, the dynamic correlation of the F atom in HF and LiF is not sufficiently captured by ΔNO-MP2 or ΔNO-CCSD. This leads to overestimation of D_e compared to exFCI (see Table II). However, the lack of static correlation in MP2 and CCSD leads to even larger overestimation of D_e.
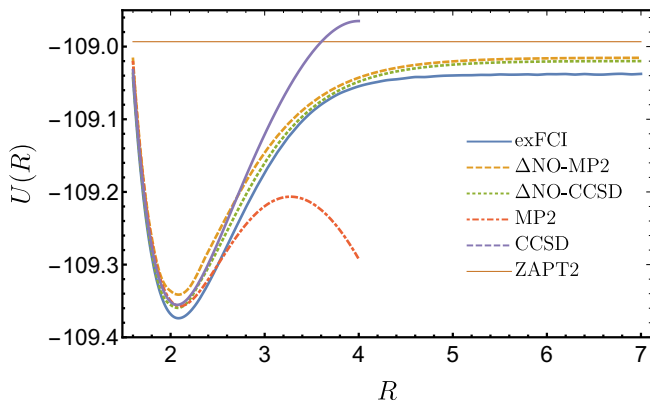
FIG. 5. Calculated N_2 potential energy curves. The ZAPT2 energy of two separate N atoms is included for comparison.

In Fig. 5, the ΔNO-MP2 and ΔNO-CCSD potential energy curves for N_2 are compared to that of MP2, CCSD and exFCI. Like F_2, ΔNO-MP2 overestimates D_e while ΔNO-CCSD underestimates it. Albeit, the amount by which the ΔNO methods are in error is somewhat greater, -24 kJ.mol^{-1} for ΔNO-MP2 and $+11$ kJ.mol^{-1} for ΔNO-CCSD. Significantly more dynamic correlation is captured by ΔNO-CCSD near equilibrium compared to ΔNO-MP2. At the exFCI equilibrium bond length, $R_e = 2.083$, $U_{\Delta\text{NO-CCSD}}(R)$ is 38 kJ.mol^{-1} above $U_{\text{exFCI}}(R)$, whereas $U_{\Delta\text{NO-MP2}}(R)$ is 85 kJ.mol^{-1} above. Both predicted equilibrium bond lengths are in good agreement with the exFCI values, particularly the ΔNO-CCSD value of $R_e = 2.084$. At dissociation, both methods underestimate the dynamic correlation by similar amounts, 60 kJ.mol^{-1} for ΔNO-MP2 and 53 kJ.mol^{-1} for ΔNO-CCSD. Interestingly, the ΔNO-MP2 energy at dissociation is 58 kJ.mol^{-1} lower than the ZAPT2 result for two separate N atoms. Analysis of the components of the ZAPT2 and ΔNO-MP2 correlation energies reveals it is the correlation between the statically correlated electrons (*i.e.*, unpaired electrons) which is responsible for this difference. Further analysis is required to fully understand and reconcile this discrepancy.

For the small collection of molecules studied, the quality of ΔNO-MP2 and ΔNO-CCSD improves, compared to the single-reference MP2 and CCSD, as the complexity of the system increases. Expectedly, as the amount of static correlation increases (*i.e.*, small R to large R, or single bond to triple bond) the ΔNO methods become significantly superior.

V. CONCLUSIONS

Combining multireference methods for static correlation with post-Hartree-Fock methods for dynamic correlation is a common approach to modeling complex electronic systems. Despite the noted success of CFT meth-

ods in modeling systems with multireference character, there is only one example of using such a method in combination with post-Hartree-Fock correlation, which is NOF-MP2. In this work, a CFT method, ΔNO, is combined with both MP2 and CCSD in a fashion completely analogous to each other. This is achieved by incorporating occupancies and vacancies, and expanded domains for occupied and virtual orbitals, according to guidelines used to derive FT-CCSD. Additionally, the MP2 and CCSD correlation energies are combined with ΔNO by inserting Δ-dependent damping factors into the residual equations. The damping factors are defined by considering the description of statically correlated electron pairs by the ΔNO 2-RDM, particularly the spin-orbitals they simultaneously occupy (and vacate) as static correlation becomes appreciable.

For the six diatomics studied, both ΔNO-MP2 and ΔNO-CCSD predict reasonable bond lengths and dissociation energies compared to the benchmark exFCI values. The error in the descriptions of HF, LiF and F_2 is largely due to the inability of MP2, or CCSD, to account for all of the dynamic correlation amongst the electrons of F. The larger error in D_e values predicted for N_2 is likely due to the fact that three bonds are being broken compared to one in the other diatomics. However, the discrepancy between the ΔNO-MP2 energy for dissociated N_2 and the ZAPT2 energy for two N atoms deserves attention. That, in combination with the discrepancy between the CCSD and ΔNO-CCSD curves for H_2, suggests that further analysis, of the modified MP2 and CCSD equations in particular, could lead to a more seamless fusion of ΔNO and post-Hartree-Fock methods.

In addition to providing an alternative treatment of multireference systems, the ΔNO-MP2 and ΔNO-CCSD methods offer insight into static and dynamic correlation and the balance between the two. Although most definitions of static correlation make use of the concept of degeneracy or near-degeneracy, the methods presented here are free from any such arguments. The damping factors are based on the simultaneous occupancy (or vacancy) of active spin-orbitals. The damping factors modify the MP2 and CCSD residual equations according to how the ΔNO static correlation influences the 2-RDM. Such concepts are relatively easy to grasp in the limit of complete static correlation, and provide a useful "physical" picture of a multireference system.

Appendix A: Amplitude damping

The MP2 and CCSD equations adopted from the finite-temperature versions [see Subsecs. II B and II C], are modified for use with the ΔNO method by incorporating a single excitation, s_i^a, and a double excitation, d_{ij}^{ab}, damping factor. The single excitation damping factor included in the CCSD r_i^a equation takes a rather simple form,

$$s_i^a = \begin{cases} 0, & \text{if } \phi_i \in \mathcal{A}, \\ 1, & \text{otherwise.} \end{cases} \quad (A1)$$

In other words, all single excitations from the active ΔNO orbitals are turned off. This arises from the assumption that single excitations are responsible for orbital relaxation,[78,79] and that the most significant part of the active orbital relaxation (due to static correlation) is obtained via the ΔNO orbital optimization.

For the double excitations, the damping is decomposed into factors for each orbital-pair,

$$d_{ij}^{ab} = d_{ij} d^{ab} d_i^a d_j^b d_i^b d_j^a. \quad (A2)$$

There are six factors to account for the six possible pairings of the four orbitals, which maintains the symmetry of the amplitudes, $t_{ij}^{ab} = -t_{ji}^{ab} = -t_{ij}^{ba} = t_{ji}^{ba}$. Rather than defining each factor in terms of a piecewise conditional function depending on the identity of the orbitals, the factors are defined here for the cases when they differ from unity [see Eqs. (A3)–(A6)]. This is when both indices correspond to active orbitals.

As in the MP2 and CCSD equations, the indices of the damping factors refer to spin-orbitals. In the ΔNO method, a spin-restricted formalism is employed and hence there are two active spin-orbitals for each active NO. The active occupied spin-orbitals are denoted by m, $\bar{m}$, n, and $\bar{n}$, where the overbar indicates spin down and the absence of an overbar indicates spin up. The active virtual orbitals are denoted by e, $\bar{e}$, f, and $\bar{f}$.

The occupied-occupied and virtual-virtual damping factors, d_{ij} and d^{ab}, are defined in a similar fashion. The form depends on whether the spin-orbitals belong to the same active NO or different active NOs. For spin-orbitals belonging to the same active NO, the damping factors are

$$d_{m\bar{m}} = \frac{1 - 2\sum_t \tau_{mt}}{n_m}, \quad d^{m\bar{m}} = \frac{1 - 2\sum_t \tau_{mt}}{h_m}, \quad (A3a)$$

$$d_{e\bar{e}} = \frac{1 - 2\sum_t \tau_{et}}{n_e}, \quad d^{e\bar{e}} = \frac{1 - 2\sum_t \tau_{et}}{h_e}. \quad (A3b)$$

As the amount of static correlation increases between electrons of the same active NO, the simultaneous occupation of both spin-orbital m and $\bar{m}$ decreases until they are ultimately unpaired at $\Delta_{me} = 1/2$ (see Fig. 1). Similarly, the corresponding virtual spin-orbitals go from empty, when there is no static correlation, to a superposition of e or $\bar{e}$ filled at $\Delta_{me} = 1/2$. The damping factors

reflect this vanishing of simultaneous opposite-spin occupancy and vacancy. When there is no static correlation ($\Delta_{me} = 0$) the damping factor is one, and when there is complete static correlation ($\Delta_{me} = 1/2$) the damping factor is zero.

For spin-orbitals belonging to different active NOs the damping factors are as follows,

$$d_{mn} = d^{mn} = \alpha_{mn}(1 + 4\kappa_{mn}), \quad (A4a)$$

$$d_{m\bar{n}} = d^{m\bar{n}} = \alpha_{mn}(1 - 4\kappa_{mn}), \quad (A4b)$$

$$d^{ef} = d_{ef} = \alpha_{ef}(1 + 4\kappa_{ef}), \quad (A4c)$$

$$d^{e\bar{f}} = d_{e\bar{f}} = \alpha_{ef}(1 - 4\kappa_{ef}), \quad (A4d)$$

$$d_{me} = d^{me} = \alpha_{me}(1 + 4\kappa_{me}), \quad (A4e)$$

$$d_{m\bar{e}} = d^{m\bar{e}} = \alpha_{me}(1 - 4\kappa_{me}), \quad (A4f)$$

where

$$\alpha_{mn} = \frac{n_m n_n - \eta_{mn}}{n_m n_n}, \quad (A5a)$$

$$\alpha_{ef} = \frac{n_e n_f - \eta_{ef}}{n_e n_f}, \quad (A5b)$$

$$\alpha_{me} = \frac{(n_m + \Delta_{me})(n_e - \Delta_{me})}{n_m n_e}. \quad (A5c)$$

Due to the HSC of the ΔNO 2-RDM, as static correlation is increased between separate electron pairs the probability the electrons of parallel-spin encounter each other increases, whereas for opposite-spin electrons it decreases (see Fig. 1). Both d_{mn} and d_{ef} increase as the amount of static correlation in both NO pairs increases ($\Delta_{me} \to 1/2$ and $\Delta_{nf} \to 1/2$). While the opposite-spin damping factors, $d_{m\bar{n}}$ and $d_{e\bar{f}}$, decrease. An analogous scenario holds true for the parallel-spin and opposite-spin vacancies (or holes), and the corresponding damping factors are therefore defined in the same manner. Each factor is also scaled by the appropriate occupancy product; occupied-occupied α_{mn}, virtual-virtual α_{ef}, or occupied-virtual α_{me}, which are taken from the pair correction to the ΔNO 2-RDM [see Eq. (11a)].

The occupied-virtual damping factors are dependent upon the simultaneous occupancy and vacancy of the active spin-orbitals. The damping factors are given by

$$d_m^e = d_e^m = 1 - 2\tau_{me} - 4\kappa_{me}, \quad (A6a)$$

$$d_m^{\bar{e}} = d_e^{\bar{m}} = 1 + 2\tau_{me} + 4\kappa_{me}, \quad (A6b)$$

$$d_m^n = d_n^m = 1 - 4\kappa_{mn}, \quad (A6c)$$

$$d_m^{\bar{n}} = d_n^{\bar{m}} = 1 + 4\kappa_{mn}, \quad (A6d)$$

$$d_e^f = d_f^e = 1 - 4\kappa_{ef}, \quad (A6e)$$

$$d_e^{\bar{f}} = d_f^{\bar{e}} = 1 + 4\kappa_{ef}, \quad (A6f)$$

$$d_m^m = d_e^e = 0, \quad (A6g)$$

$$d_m^{\bar{m}} = d_e^{\bar{e}} = 0. \quad (A6h)$$

Similar to the occupied-occupied and virtual-virtual damping factors, the occupied-virtual damping factor decreases or increases (with static correlation) depending

on the spin pairing. Unlike the previous damping factors, the occupied-virtual damping factor decreases for orbitals of parallel spin and increases for opposite spin. This is due to the inverse nature of vacancy compared to occupancy (*i.e.*, when the spin-up orbital is occupied the spin-down orbital is vacant, and vice versa). Furthermore, the damping factor associated with excitations from an active orbital (occupied or virtual) to the same active orbital is set to zero.

Finally, if all indices correspond to active spin-orbitals, then the damping factor is zero, *i.e.*,

$$d_{mn}^{ef} = 0, \quad \text{if } \phi_m \wedge \phi_n \wedge \phi_e \wedge \phi_f \in \mathcal{A}. \tag{A7}$$

It is assumed that such interactions are already included in the ΔNO 2-RDM.

[1] D. K. W. Mok, R. Neumann, and N. C. Handy, J. Phys. Chem. **100**, 6225 (1996).
[2] N. C. Handy and A. J. Cohen, Mol. Phys. **99**, 403 (2001).
[3] D. Cremer, Mol. Phys. **99**, 1899 (2001).
[4] A. D. Becke, J. Chem. Phys. **138**, 074109 (2013).
[5] D. L. Crittenden, J. Phys. Chem. A **117**, 3852 (2013).
[6] T. Tsuchimochi and T. V. Voorhis, J. Chem. Phys. **141**, 164117 (2014).
[7] A. J. Wallace and D. L. Crittenden, J. Phys. Chem. A **118**, 2138 (2014).
[8] J. W. Hollett, H. Hosseini, and C. Menzies, J. Chem. Phys. **145**, 084106 (2016).
[9] E. Ramos-Cordoba, P. Salvador, and E. Matito, Phys. Chem. Chem. Phys. **18**, 24015 (2016).
[10] C. L. Benavides-Riveros, N. N. Lathiotakis, and M. A. L. Marques, Phys. Chem. Chem. Phys. **19**, 12655 (2017).
[11] M. Via-Nadal, M. Rodriguez-Mayorga, E. Ramos-Cordoba, and E. Matito, J. Phys. Chem. Lett. **10**, 4032 (2019).
[12] E. Fromager, J. Toulouse, and H. Jørgen Aa. Jensen, J. Chem. Phys. **126**, 074111 (2007).
[13] J. Toulouse, I. C. Gerber, G. Jansen, A. Savin, and J. G. Angyán, Phys. Rev. Lett. **102**, 096404 (2009).
[14] B. G. Janesko, T. M. Henderson, and G. E. Scuseria, J. Chem. Phys. **130**, 081105 (2009).
[15] J.-D. Chai and M. Head-Gordon, J. Chem. Phys. **131**, 174105 (2009).
[16] A. Stoyanova, A. M. Teale, J. Toulouse, T. Helgaker, and E. Fromager, J. Chem. Phys. **139**, 134113 (2013).
[17] J. Cizek, Adv. Chem. Phys. **14**, 35 (1969).
[18] B. Jeziorski and H. J. Monkhorst, Phys. Rev. A **24**, 1668 (1981).
[19] K. Andersson, P. Malmqvist, B. O. Roos, A. J. Sadlej, and K. Wolinski, J. Phys. Chem. **94**, 5483 (1990).
[20] P. Pulay, Int. J. Quantum Chem. **111**, 3273 (2011).
[21] F. A. Evangelista, J. Chem. Phys. **149**, 030901 (2018).
[22] E. R. Sayfutyarova, Q. Sun, G. K.-L. Chan, and G. Knizia, J. Chem. Theory Comput. **13**, 4063 (2017).
[23] J. J. Bao, S. S. Dong, L. Gagliardi, and D. G. Truhlar, J. Chem. Theory Comput. **14**, 2017 (2018).
[24] P. G. Szalay, T. Müller, G. G. abd H. Lischka, and R. Shepard, Chem. Rev. **112**, 108 (2012).
[25] D. I. Lyakh, M. Musial, V. F. Lotrich, and R. J. Bartlett, Chem. Rev. **112**, 182 (2012).
[26] A. Köhn, M. Hanauer, L. A. Mück, T.-C. Jagau, and J. Gauss, WIREs Comput. Mol. Sci. **3**, 176 (2013).
[27] K. Andersson, P. Malmqvist, and B. O. Roos, J. Chem. Phys. **96**, 1218 (1992).
[28] T. Shiozaki, W. Györffy, P. Celani, and H.-J. Werner, J. Chem. Phys. **135**, 081106 (2011).
[29] C. Angeli, R. Cimiraglia, S. Evangelisti, T.Leininger, and J. Malrieu, J. Chem. Phys. **114**, 10252 (2001).
[30] C. Angeli, R. Cimiraglia, and J. Malrieu, Chem. Phys. Lett. **350**, 297 (2001).
[31] C. Angeli, R. Cimiraglia, and J. Malrieu, J. Chem. Phys. (2002).
[32] M. Hoffmann and Y. G. Khait, Chem. Phys. Lett. **311**, 372 (1999).
[33] D. I. Lyakh, V. V. Ivanov, and L. Adamowicz, J. Chem. Phys. **122**, 024108 (2005).
[34] A. J. W. Thom and M. Head-Gordon, J. Chem. Phys. **131**, 124113 (2009).
[35] S. R. Yost, T. Kowalczyk, and T. Van Voorhis, J. Chem. Phys. **139**, 174104 (2013).
[36] E. J. Sundstrom and M. Head-Gordon, J. Chem. Phys. **140**, 114103 (2014).
[37] H. G. A. Burton and A. J. W. Thom, J. Chem. Theory Comput. (ASAP article).
[38] T. L. Gilbert, Phys. Rev. B **12**, 2111 (1975).
[39] G. Zumbach and K. Maschke, J. Chem. Phys. **82**, 5604 (1985).
[40] W. Kutzelnigg, J. Chem. Phys. **125**, 171101 (2006).
[41] A. Y. Sokolov and H. F. Schaefer III, J. Chem. Phys. **139**, 204110 (2013).
[42] L. M. Mentel, R. van Meer, O. V. Gritsenko, and E. J. Baerends, J. Chem. Phys. (2014).
[43] R. van Meer, O. V. Gritsenko, and E. J. Baerends, J. Chem. Phys. **148**, 104102 (2018).
[44] C. Schilling, J. Chem. Phys. **149**, 231102 (2018).
[45] J. Schmidt, C. L. Benavides-Riveros, and M. A. L. Marques, Phys. Rev. B **99**, 224502 (2019).
[46] A. M. K. Müller, Phys. Lett. A **105**, 446 (1984).
[47] S. Goedecker and C. J. Umrigar, Phys. Rev. Lett. **81**, 866 (1998).
[48] D. R. Rohr, K. Pernal, O. V. Gritsenko, and E. J. Baerends, J. Chem. Phys. **129**, 164105 (2008).
[49] M. Piris and P. Otto, Int. J. Quantum Chem. **94**, 317 (2003).
[50] P. Leiva and M. Piris, J. Chem. Phys. **123**, 214102 (2005).
[51] M. Piris, Int. J. Quantum Chem. **113**, 620 (2012).
[52] M. Piris, J. Chem. Phys. **141**, 044107 (2014).
[53] M. Piris, Phys. Rev. Lett. **119**, 063002 (2017).
[54] M. Piris, Phys. Rev. A **98**, 022504 (2018).
[55] A. F. White and G. K.-L. Chan, J. Chem. Theory Comput. **14**, 5690 (2018).
[56] M. Kobayashi and T. Taketsugu, Theor. Chem. Acc. **134**, 107 (2015).
[57] R. Santra and J. Schirmer, Chem. Phys. **482**, 355 (2017).
[58] W. Kutzelnigg and D. Mukherjee, J. Chem. Phys. **110**, 2800 (1999).
[59] L. Bytautas, T. M. Henderson, C. A. Jiménez-Hoyos, J. K. Ellis, and G. E. Scuseria, J. Chem. Phys. **135**, 044119 (2011).
[60] W. Polemans, M. Van Raemdonck, B. Verstichel, S. De Baerdemacker, A. Torre, L. Lain, G. E. Massaccesi, D. R. Alcoba, P. Bultinck, and D. Van Neck, J. Chem. Theory Comput. **11**, 4064 (2015).
[61] J. F. Stanton, J. Gauss, J. D. Watts, and R. J. Bartlett, J. Chem. Phys. **94**, 4334 (1991).
[62] P. Pulay and S. Saebø, Theor. Chim. Acta **69**, 357 (1986).
[63] B. Huron, J.-P. Malrieu, and P. Rancurel, J. Chem. Phys. **58**, 5745 (1973).
[64] E. Giner, A. Scemama, and M. Caffarel, Can. J. Chem. **91**, 879 (2013).
[65] E. Giner, A. Scemama, and M. Caffarel, J. Chem. Phys. **142**, 044115 (2015).
[66] Y. Garniron, A. Scemama, P.-F. Loos, and M. Caffarel, J. Chem. Phys. **147**, 034101 (2017).
[67] P.-F. Loos, A. Scemama, A. Blondel, Y. Garniron, M. Caffarel, and D. Jacquemin, J. Chem. Theory Comput. **14**, 4360 (2018).
[68] Y. Garniron, K. Gasperich, T. Applencourt, A. Benali, A. Ferte, J. Paquier, B. Pradines, R. Assaraf, P. Reinhardt, J. Toulouse, P. Barbaresco, N. Renon, G. David, J. P. Malrieu, M. Veril, M. Caffarel, P. F. Loos, E. Giner, and A. Scemama, J. Chem. Theory Comput. **15**, 3591 (2019).
[69] T. H. Dunning Jr., J. Chem. Phys. **90**, 1007 (1989).
[70] B. P. Prascher, D. E. Woon, K. A. Peterson, T. H. Dunning, and

A. K. Wilson, Theor. Chem. Acc. **128**, 69 (2011).

[71] D. Feller, J. Comput. Chem. **17**, 1571 (1996).

[72] K. L. Schuchardt, B. T. Didier, T. Elsethagen, L. Sun, V. Gurumoorthi, J. Chase, J. Li, and T. L. Windus, J. Chem. Inf. Model. **47**, 1045 (2007).

[73] R. A. Poirier, J. W. Hollett, and P. L. Warburton, MUNgauss. Memorial University, Chemistry Department, St. John's, NL A1B 3X7 (2015), with contributions from A. Alrawashdeh, J.-P. Becker, J. Besaw, S.D. Bungay, F. Colonna, A. El-Sherbiny, T. Gosse, D. Keefe, A. Kelly, D. Nippard, C.C. Pye, D. Reid, K.

Saputantri, M. Shaw, M. Staveley, O. Stueker, Y. Wang, and J. Xidos.

[74] M. Piris and J. M. Ugalde, J. Comput. Chem. **30**, 2078 (2009).

[75] P. Pulay, J. Comput. Chem. **3**, 556 (1982).

[76] G. E. Scuseria, T. J. Lee, and H. F. Schaefer III, Chem. Phys. Lett. **130**, 236 (1986).

[77] T. J. Lee and D. Jayatilaka, Chem. Phys. Lett. **201**, 1 (1993).

[78] G. E. Scuseria and H. F. Schaefer, Chem. Phys. Lett. **142**, 354 (1987).

[79] C. D. Sherrill, A. I. Krylov, E. F. C. Byrd, and M. Head-Gordon, J. Chem. Phys. **109**, 4171 (1998).